MOLECULAR AND CELLULAR BIOLOGY, Aug. 2010, p. 3981–3993 Vol. 30, No. 16
0270-7306/10/$12.00 doi:10.1128/MCB.01284-09

Mitochondrial *HEP27* Is a c-Myb Target Gene That Inhibits Mdm2 and Stabilizes p53▽†

Chad Deisenroth,[1,2,5] Aaron R. Thorner,[1,2,3] Takeharu Enomoto,[7] Charles M. Perou,[2,3,6] and Yanping Zhang[1,2,4,5]*

Curriculum in Genetics and Molecular Biology, University of North Carolina at Chapel Hill, Chapel Hill, North Carolina[1]; Lineberger Comprehensive Cancer Center, School of Medicine, University of North Carolina at Chapel Hill, Chapel Hill, North Carolina[2]; Department of Genetics, University of North Carolina at Chapel Hill, Chapel Hill, North Carolina[3]; Department of Pharmacology, School of Medicine, University of North Carolina at Chapel Hill, Chapel Hill, North Carolina[4]; Department of Radiation Oncology, School of Medicine, University of North Carolina at Chapel Hill, Chapel Hill, North Carolina[5]; Department of Pathology and Laboratory Medicine, University of North Carolina at Chapel Hill, Chapel Hill, North Carolina[6]; and Department of Gastoenterological and General Surgery, St. Marianna University School of Medicine, 2-16-1 Sugao, Miyamae, Kawasaki, Kanagawa, Japan[7]

Received 23 September 2009/Returned for modification 1 December 2009/Accepted 4 June 2010

The ever-expanding knowledge of the role of p53 in cellular metabolism, apoptosis, and cell cycle control has led to increasing interest in defining the stress response pathways that regulate Mdm2. In an effort to identify novel Mdm2 binding partners, we performed a large-scale immunoprecipitation of Mdm2 in the osteosarcoma U2OS cell line. One significant binding protein identified was Hep27, a member of the short-chain alcohol dehydrogenase/reductase (SDR) family of enzymes. Here, we demonstrate that the Hep27 preprotein contains an N-terminal mitochondrial targeting signal that is cleaved following mitochondrial import, resulting in mitochondrial matrix accumulation of mature Hep27. A fraction of the mitochondrial Hep27 translocates to the nucleus, where it binds to Mdm2 in the central domain, resulting in the attenuation of Mdm2-mediated p53 degradation. In addition, Hep27 is regulated at the transcriptional level by the proto-oncogene c-Myb and is required for c-Myb-induced p53 stabilization. Breast cancer gene expression analysis correlated estrogen receptor (ER) status with Hep27 expression and p53 function, providing a potential *in vivo* link between estrogen receptor signaling and p53 activity. Our data demonstrate a unique c-Myb-Hep27-Mdm2-p53 mitochondria-to-nucleus signaling pathway that may have functional significance for ER-positive breast cancers.

The Mdm2-p53 stress response pathway is an important regulator of cellular homeostasis. A variety of mitogenic and genotoxic stressors converge on this pathway to elicit a protective p53-dependent stress response resulting in cell cycle arrest, apoptosis, DNA repair, or replicative senescence (23). There are a number of posttranslational regulators that modify the capacity of Mdm2 to control p53 levels. In response to DNA damage, Mdm2 itself is a target for phosphorylation by protein kinases ATM (26) and DNA-PK (27), leading to inhibition of the Mdm2-p53 protein interaction and subsequent p53 stabilization. A number of cellular proteins, including Myc, Ras, and E2F1, when overexpressed or constitutively active, can promote p53 stabilization via the inhibition of Mdm2 by the tumor suppressor p19Arf (47). Most recently, the ribosomal proteins L5, L11, and L23 have all been reported to respond to alleged nucleolar stress by binding to and inhibiting the ability of Mdm2 to promote p53 turnover (6, 18, 25, 61).

Hep27, or dehydrogenase/reductase member 2 (gene name, *DHRS2*), was originally identified as a nuclear protein in the sodium butyrate-treated human hepatocellular carcinoma cell line HepG2 (8, 12). Sequence alignment of Hep27 reveals considerable evolutionary conservation from plants to humans (46), with significant homology to *s*hort-chain alcohol *d*ehydrogenase/*r*eductase (SDR) enzymes; a superfamily of primarily NAD/NAD(P)-dependent oxidoreductases involved in a host of intermediate metabolic processes (19). Further characterization of Hep27 revealed a gene localized to chromosome 14q11.2 (36), a region characterized by high-frequency loss of heterozygosity in a number of different tumor types, including nasopharyngeal carcinoma (4, 29), malignant mesothelioma (3), gastrointestinal stromal tumors (7, 10), and metastatic lung adenocarcinomas (13). The correlation of Hep27 expression with both inhibition of cell proliferation (12) and cellular quiescence (37), as well as locus-specific deletion in a number of cancer types, supports the notion that Hep27 has a functional role in promoting growth inhibition.

The proto-oncogene c-Myb was identified as the mammalian homolog of v-Myb, an oncogene identified in the avian leukemia viruses avian myeloblastosis virus (AMV) and E26. c-Myb is a member of the Myb family of transcription factors and has been implicated in cellular processes of proliferation and differentiation (30). c-Myb gene amplification and overexpression has been documented for a number of leukemia subtypes,

* Corresponding author. Mailing address: University of North Carolina at Chapel Hill, Department of Radiation Oncology, School of Medicine, Box 7512, 101 Manning Drive, Chapel Hill, NC 27514. Phone: (919) 445-5287. Fax: (919) 966-7681. E-mail: ypzhang@med.unc.edu.

† Supplemental material for this article may be found at http://mcb.asm.org/.

▽ Published ahead of print on 14 June 2010.

colorectal cancer, and breast cancer (reviewed in reference 40). Identifying and confirming a common set of c-Myb target genes has remained an arduous task, with results showing little commonality among the various cell types and experimental approaches (2, 22, 40), suggesting that specific targets may be context dependent (31). Efforts to identify common c-Myb target genes have stratified genes into three general ontologies: those involved with housekeeping functions, genes implicated in specific differentiated lineages, and genes involved in cell proliferation and survival (40).

Here, we report that Hep27 is a bona fide target gene of c-Myb in cell types with detectable Hep27 expression. As a mitochondrial matrix protein, Hep27 can be actively imported to the mitochondria via an N-terminal mitochondrial targeting signal. Cleavage of the mitochondrial targeting signal produces a mature form of Hep27, which is then capable of translocating to the nucleus, where it binds to the central domain of Mdm2, thereby promoting p53 accumulation and stabilization. Consistent with a role for p53 in monitoring sustained oncogenic activity, elevated c-Myb activity can enhance Hep27 expression levels, resulting in greater nuclear accumulation of Hep27 and, therefore, increased p53 stabilization. In addition, probing large gene expression datasets of human breast tumor samples revealed a potential link between estrogen receptor (ER), c-Myb, Hep27, and wild-type p53 in the luminal A tumor subtype. Thus, we propose a novel c-Myb-Hep27-Mdm2-p53 pathway that utilizes the extramitochondrial tumor suppressor function of Hep27 to modulate basal p53 function, which has potential implications for ER-positive (ER^+) luminal breast cancers.

MATERIALS AND METHODS

Cell culture and reagents. U2OS, H1299, MCF-7, HepG2, and WI-38 cell lines were maintained in Dulbecco's modified Eagle's medium supplemented with 10% fetal bovine serum, L-glutamine, 100 U/ml penicillin, and 100 μg/ml streptomycin at 5% CO_2 in a humidified chamber. Cell transfections were carried out with Fugene 6 (Roche), Fugene HD (Roche), or Effectene (Qiagen) reagents. Sodium butyrate and MG132 were both obtained from Sigma.

Plasmids and adenovirus. To generate a human Hep27 expression construct, the full-length Hep27 cDNA (Open Biosystems) was amplified by PCR and cloned into the pcDNA3 expression vector (Invitrogen). pcDNA3-Flag vector was used to construct full-length Hep27 and the deletion mutant Hep27-DelN24. pcDNA3-Myc was used to construct N-terminally tagged Hep27 and Mdm2 truncation mutants. pEGFP-NI (Clontech) was used to generate the green fluorescent protein (GFP) fusion protein HepMTS-GFP. pGL3-Basic (Promega) was used for luciferase reporter constructs. The ADEASY XL system (Stratagene) was used for creating adenovirus. DNA sequences were subcloned into pShuttle-CMV, recombined with pADEASY-1 vector, and transfected into 293 QBT cells to generate adenovirus.

RNAi. Oligofectamine reagent (Invitrogen) was used for transfection of oligonucleotides for RNA interference (RNAi). The Hep27 sequences (Invitrogen) targeting the 3′ end of the coding sequence were RNAi 1, 5′-GGAACAUCAU CAGCUGCAGAGGAUU, and RNAi 2, 5′-CCUGGUCUCUUCCAUUGCA GCUUAU. Stable short hairpin RNA (shRNA) MCF-7 lines were created expressing either pRS-shMyb (5′-CGTTGGTCTGTTATTGCCAAGCACTTA AA-3′) or pRS-shGFP (5′-TGACCACCCTGACCTACGGCGTGCAGTGC-3′) (catalog no. TR311329; Origene, Rockville, MD). Briefly, Phoenix 293T packaging cells were transfected with 10 μg of retroviral cassette (pRS-shMyb or pRS-shGFP) using Lipofectamine 2000 (Invitrogen, Carlsbad, CA) according to the manufacturer's instructions. The medium was changed 24 h posttransfection, and supernatant collected after 12 h. MCF-7 cells were transduced by applying supernatants plus 75 μg Polybrene. Stable populations were obtained by culturing in 2 μg/ml puromycin for 2 weeks and keeping them under constant selection thereafter. After 2 weeks, cells from the MCF-7 pRS-shMyb line were plated at clonal density and >20 clones chosen to analyze for efficient knockdown. Clones with the greatest knockdown were kept for further analysis.

TEM. Cells grown on chamber slides were fixed with 4% paraformaldehyde in 0.15 M sodium phosphate, pH 7.4, for 1 h. Using a preembedding immunogold/silver-staining protocol (59), cells were incubated in a 1:50 dilution of rabbit anti-Hep27, followed by the secondary antibody incubation in goat anti-rabbit IgG 0.8-nm immunogold (Aurion; Electron Microscopy Sciences). After silver enhancement, the cells were processed and embedded in Polybed 812 epoxy resin (Polysciences, Inc., Warrington, PA). Ultrathin 70-nm sections were cut, mounted on copper grids, and poststained with 4% uranyl acetate and Reynolds' lead citrate. Sections were observed using a LEO EM-910 transmission electron microscope (TEM) operating at 80 kV (LEO Electron Microscopy, Thornwood, NY), and images were taken using a Gatan Orius SC1000 charge-coupled device (CCD) camera with Digital Micrograph 3.11.0 (Gatan, Inc., Pleasanton, CA).

Immunofluorescence. Monolayer cells were fixed with formaldehyde, permeabilized by using 0.2% Triton X-100, and targeted with primary anti-Hep27 or anti-Flag M2 antibody. Goat anti-rabbit rhodamine red-, Cy2-, fluorescein isothiocyanate-, and 7-amino-4-methylcoumarin-3-acetic acid (AMCA)-conjugated secondary antibodies were purchased commercially (Jackson ImmunoResearch Laboratories). Mitotracker red CMXRos (Invitrogen) was used for mitochondrial staining, and DAPI (4′,6-diamidino-2-phenylindole) was used for nuclear demarcation. Immunostained cells were analyzed using an Olympus IX-81 microscope fitted with a SPOT camera and software.

Antibodies. For generation of affinity-purified anti-Hep27 antibody, peptides corresponding to amino acid residues 43 to 57 and 213 to 227 (peptide 213–227) were used as antigens to immunize rabbits. To test for seroconversion, rabbits were bled from the ear vein and the sera tested against U2OS whole-cell lysates in a Western blot assay (data not shown). Peptide 213–227 provided the greatest specificity, and therefore, subsequent bleeds from this rabbit were used to generate antiserum for use in Western blot assays, immunoprecipitation of Hep27-Mdm2 complexes, and immunocytochemistry.

The following antibodies were commercially purchased: mouse anti-Mdm2 4B11, 2A10, and SMP14 (UNC Tissue Culture and Molecular Biology Support Facility), mouse antiactin (Neomarkers), mouse anti-p53 DO.1 (Neomarkers), rabbit anti-GRP75 H-155 (Santa Cruz), rabbit anti-histone H3 9715 (Cell Signaling), mouse anti-Flag M2 (Sigma), and rabbit anti-c-Myb 45150 (Abcam). Rabbit anti-p21 and rabbit anti-Myc were kindly provided by Yue Xiong.

Luciferase assay. The primers used to amplify regions of interest from U2OS genomic DNA were P1 FOR and REV (5′-AGAGGTGAAGCCGGCTG and 5′-GCTGCCGGCTCAGGCAG), P1DelB FOR and REV (5′-AGAGGTGAA GCCGGCTG and 5′-ATCCTGCTGATTGGTCC), P1DelAB FOR and REV (5′-AGAGGTGAAGCCGGCTG and 5′-GTGCTGATTGGTGCATTTAC), and P1AB FOR and REV (5′-TCTGTCAAAACGGACCAATC and 5′-GCTG CCGGCTCAGGCAG). PCR fragments were subcloned into the pGL3-Basic luciferase reporter plasmid.

For site-directed mutagenesis, regions of the conserved Myb response element (MRE) [(C/T)AAC(G/T)G] were deleted from the predicted MRE A and MRE B Myb binding sites using a QuikChange II site-directed mutagenesis kit (Stratagene). For MRE A (5′-AAACGG, plus strand, nucleotides −143 to −138), nucleotides −142 to −140 were deleted and a T added 3′ of nucleotide −138 to create a KpnI site. For MRE B (5′-TAACTG, minus strand, nucleotides −39 to −34), nucleotides −38 to −33 were deleted and a C added 3′ of nucleotide −39 to create a SmaI site. Confirmation of deletion was confirmed by successful cleavage of the respective incorporated restriction site, followed by DNA sequencing of positive clones.

Reporter constructs were transfected into H1299 cells for 48 h to detect luciferase and β-galactosidase activity using the Dual-Light system (Applied Biosystems). Assays were run in 96-well-plate format on an Lmax microplate luminometer (Molecular Devices). Relative light units were normalized by the luciferase activity/β-galactosidose ratio.

Biochemical fractionations. An optimized differential detergent fractionation procedure was utilized as previously described (41).

Quantitative reverse transcription (qRT)-PCR. RNA was purified from WI-38 cells using an RNeasy mini kit (Qiagen). SYBR green PCR master mix (Applied Biosystems) was combined with primers targeting exons 1 and 2 of Hep27. The primers used were 5′-AAGACCACGAATGCACCGAGAG (forward) and 5′-GGCAACTGCTGACAGCATAGTGG (reverse). Relative Hep27 mRNA levels were normalized with glyceraldehyde-3-phosphate dehydrogenase (GAPDH) as the internal control.

Microarray statistical analysis. Human breast tumor microarray data from a Swedish patient cohort ($n = 236$) was used for all tumor analyses (28). Tumors were classified into intrinsic breast cancer subtypes using the PAM50 classifier exactly as described in reference 35. Disease-specific survival by subtype was

visualized by a Kaplan-Meier survival plot and tested for significance using the chi-square test (WinSTAT version 2007.1). Association of c-Myb or Hep27 expression with breast cancer subtypes, estrogen receptor status ($n = 232$), or p53 mutation status was tested for statistical significance by analysis of variance (ANOVA) using the R system for statistical computing (R Development Core Team, 2006; http://www.R-project.org). A 52-gene signature capable of predicting nonfunctional p53 (i.e., p53 mutation signature) was applied to the data set of Miller et al. (28) as done previously (56). The distribution of the p53 mutation signature across tumor subtypes was visualized by a box-and-whisker plot, and statistical significance calculated by ANOVA.

RESULTS

Hep27 is a mitochondrial matrix protein. In an effort to identify novel Mdm2 binding partners, a large-scale immunoprecipitation (IP) experiment was performed using Mdm2 as bait in the osteosarcoma U2OS cell line. An adenovirus construct expressing wild-type Mdm2 was used to infect U2OS cells. The IP was resolved by SDS-PAGE and silver stained, and bands of interest not found in the adenovirus GFP control sample were subjected to mass spectrometry protein microsequencing (Fig. 1A). The large ribosomal proteins L5, L11, and L23, previously reported to bind to Mdm2 through IP, also appeared in this pulldown. A fourth prominent band, migrating just below the IgG light chain (IgG-L) with an apparent molecular mass of 24 kDa, was identified as Hep27.

Hep27 was originally described as a predicted 27-kDa protein residing within the nucleus of HepG2 cells following treatment with the histone deacetylase inhibitor sodium butyrate, a drug that induces a reversible G_1 cell cycle arrest. Further analysis reporting the full coding sequence of Hep27 described a protein with 280 amino acids (12) that could be detected as two different bands by Western blot assay (36). The recombinant cDNA sequence predicts a protein of 280 amino acids with a mass of 29.9 kDa. However, initial N-terminal peptide sequencing of purified Hep27 revealed a truncated protein beginning at Ser24 with a predicted mass of 27.3 kDa (12). The truncated form of Hep27 is the predominant band in most cell types and tissues we and others have surveyed (data not shown). It is also the form that was detected migrating just below the 25-kDa marker in our Mdm2 screen in U2OS cells. We consistently detect Hep27 at this position in HepG2, U2OS, and MCF7 cells, three cell lines that express Hep27. Therefore, we conclude that the 24-kDa Hep27 identified by mass spectrometry in our experiments is Hep27 (isoform 2) and reflects the same protein reported in previous literature.

Previous reports have described Hep27 as a nuclear protein with prominent cytoplasmic localization (12); however, computational algorithms predicted mitochondrial localization (5, 11). To gain direct insight into Hep27 localization, a polyclonal antibody was raised against a short peptide near the C terminus (VVPGIIKTDFSKVFH). The fluorescent immunostaining pattern of Hep27 exhibited striated perinuclear staining, consistent with possible mitochondrial localization (Fig. 1B). To verify this, the cells were simultaneously probed with Mitotracker red CMXRos, a marker selective for mitochondrial staining. An image merging these results demonstrates that endogenous Hep27 colocalizes with mitochondria in U2OS cells (Fig. 1B).

In general, nuclear-derived gene products destined for the mitochondria must undergo import via the *t*ranslocase of the *o*uter *m*embrane (Tom) complex embedded in the mitochondrial outer membrane (57). The Tom20 import receptor facilitates the import of proteins containing mitochondrial targeting signals (MTS) (38). Initial reports of Hep27 described a protein beginning at Ser24, consistent with amino acids 1 to 23 comprising a putative MTS that is later cleaved during processing (see Fig. S1 in the supplemental material). To examine the role of this possible MTS in Hep27, we created an N-terminal deletion mutant by removing the first 24 amino acids (Hep27-DelN24-Flag) and assessed mitochondrial exclusion by immunofluorescence staining. Full-length Hep27 retains a predominantly mitochondrial localization, whereas Hep27-DelN24 exhibits no obvious perinuclear staining and does not overlie the mitochondrial marker (Fig. 1C). To further assess the functional nature of the MTS, the DNA sequence corresponding to amino acids 1 to 24 of Hep27 was cloned into pEGFP-N1 to generate HepMTS-GFP; a fusion protein containing the potential MTS of Hep27 at the N terminus of enhanced GFP (EGFP). Control GFP expression in U2OS cells is distributed equally throughout the cytosol and nucleus of the cell, with no visible entry into the mitochondria (Fig. 1D). However, HepMTS-GFP exhibits a perinuclear pattern similar to that of endogenous Hep27 and colocalizes well with Mitotracker staining, indicating efficient import of HepMTS-GFP to the mitochondria. Once imported into the matrix space, the MTS is cleaved off to generate mature Hep27 (see Fig. S2A and B in the supplemental material). These data suggest that the N-terminal 24 amino acids of Hep27 are both sufficient and necessary to direct mitochondrial import of Hep27.

To further solidify Hep27 as a mitochondrial protein, a differential detergent fractionation (DDF) procedure (41) was optimized to partition out mitochondrial proteins. Three independent replicates of DDF performed on endogenous protein in U2OS cells demonstrated Hep27 accumulating with heat shock protein 70 (Hsp70) in the mitochondrial fraction and not with the cytoplasmic fraction (Fig. 1E).

Immunogold labeling of endogenous Hep27 in U2OS cells for visualization by transmission electron microscopy (TEM) illustrates a staining pattern enriched within mitochondria, with gold particle distribution appearing randomly throughout the organelle (Fig. 1F). A higher-magnification micrograph with a transverse cross-section of a mitochondrion shows Hep27 labeling randomly distributed throughout the matrix space, with little concentration in the intermembrane space or membrane regions (see Fig. S3 in the supplemental material). Together with direct mitochondrial import and cleavage of a mitochondrial targeting signal, the evidence supports the predominant localization of Hep27 in the mitochondrial matrix.

Hep27 partially localizes to the nucleus. A number of mitochondrial proteins, including Hsp60 and p32, have been reported to be partially localized to extra-mitochondrial locations to perform nonmitochondrial functions (51). Since Hep27 was initially reported as a nuclear protein (12), we assessed the possible nuclear localization of Hep27 by visualizing endogenous Hep27 in U2OS via TEM. There is detectable nuclear distribution of gold particle-labeled Hep27 within the nuclei (Fig. 2A). These findings are corroborated by the results of subcellular fractionation of U2OS cells (Fig. 2B), in which the majority of Hep27 is found within the mitochondria, as expected, but a minor fraction accumulates within the nu-

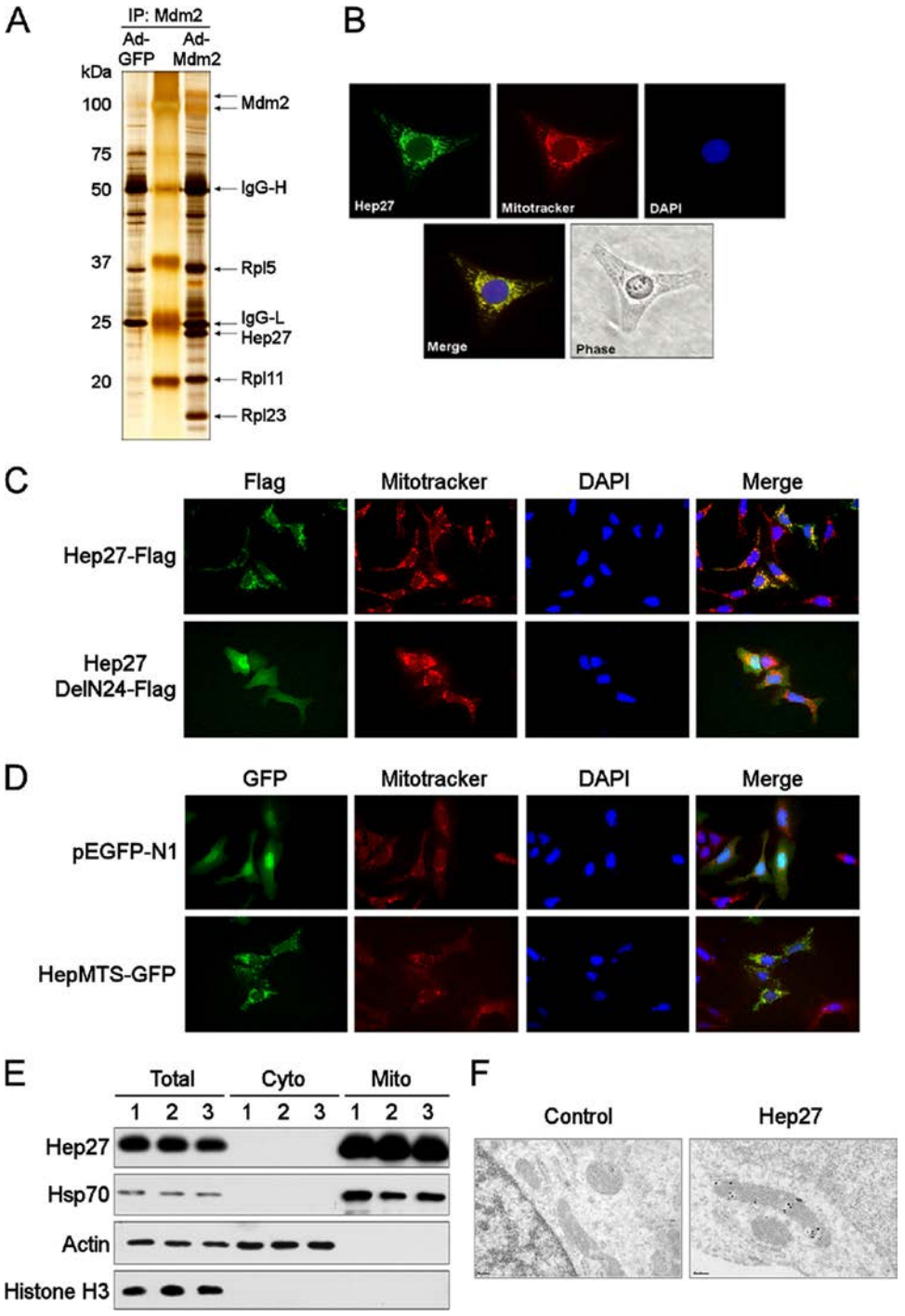

FIG. 1. Hep27 is a mitochondrial matrix protein. (A) U2OS cells infected by adenovirus (Ad) expressing control GFP or Mdm2 for 24 hours were immunoprecipitated with anti-Mdm2 2A10 antibody and resolved by SDS-PAGE. Hep27 was identified by mass spectrometry protein microsequencing analysis. First lane, Ad-GFP; second lane, protein ladder; third lane, Ad-Mdm2. (B) Immunofluorescence imaging of endogenous Hep27. U2OS cells were probed with anti-Hep27 antibody, Mitotracker CMXRos, and DAPI. Phase, phase-contrast image. (C) Expression constructs expressing full-length C-terminal Flag-tagged Hep27 or Hep27-DelN24 were transfected into U2OS cells. Anti-Flag M2 antibody was used to detect the flag-tagged protein. Mitotracker CMXRos was used to visualize mitochondria, and DAPI was used for nuclear staining. (D) Expression constructs expressing control GFP or HepMTS-GFP fusion protein were transfected into U2OS cells. Mitotracker CMXRos was used to visualize the mitochondria, and DAPI for nuclear staining. (E) Differential detergent fractionation was performed in triplicate in U2OS cells to fractionate endogenous Hep27. Hsp70 is the mitochondrial control, actin is the cytosolic control, and histone H3 is the nuclear control. Cyto, cytosolic compartment; Mito, mitochondrial compartment. (F) Transmission electron microscopy of endogenous Hep27 in U2OS cells. U2OS monolayers were fixed, probed with control IgG antibody (left) or anti-Hep27 primary antibody (right), and visualized by TEM.

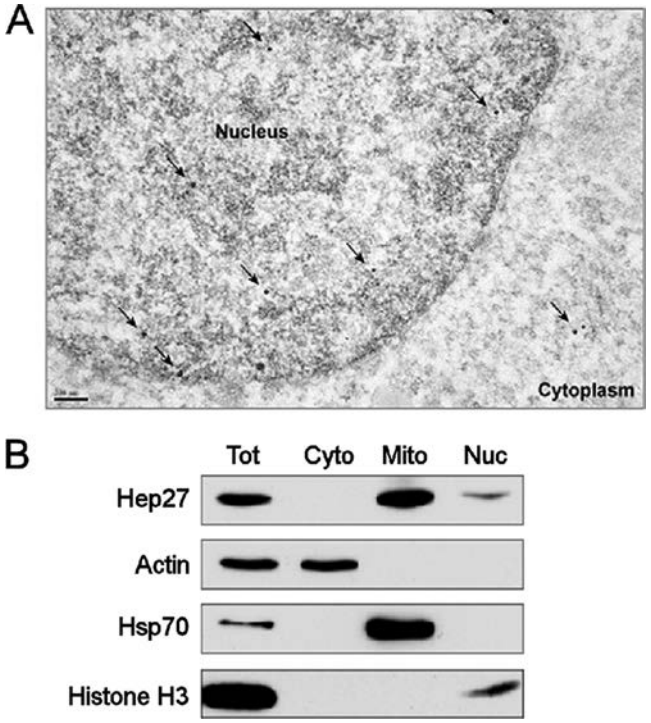

FIG. 2. Hep27 partially localizes to the nucleus. (A) U2OS cell monolayers were fixed and probed for endogenous Hep27 with anti-Hep27 antibody. Arrows denote gold bead-labeled Hep27 as detected by TEM. (B) Differential detergent fractionation was used to fractionate endogenous total (Tot) Hep27 from U2OS cells into the cytosolic (Cyto), mitochondrial (Mito), and nuclear (Nuc) compartments for detection by Western blot assay. Actin, Hsp70, and histone H3 were used as cytosolic, mitochondrial, and nuclear controls, respectively.

cleus. These findings together provide evidence that, once processed in the mitochondrial matrix, a minor fraction of Hep27 translocates from the mitochondria to the nucleus. It should be noted that while Hep27 is abundantly expressed in U2OS cells, processing of Hep27 to the mature form can only occur in the mitochondrial matrix, indicating that the minor fraction of Hep27 located within the nucleus must be translocated from the mitochondria to the nucleus.

Hep27 binds to Mdm2. Given that Hep27 was pulled out of an Mdm2 screen for binding partners, we sought to determine the validity of this binding interaction. A coupled transcription/translation system was used to synthesize [^{35}S]methionine-labeled human Mdm2 and Hep27-Flag. Immunoprecipitations were performed using a monoclonal mouse antibody to Mdm2 (4B11) or an anti-Flag monoclonal antibody. Mdm2 and Hep27 can bind in reciprocal fashion in a cell-free system (Fig. 3A). For further investigation into binding dynamics of Mdm2 and Hep27, we utilized constructs expressing Mdm2 and Myc-tagged Hep27 which were coexpressed by transient transfection in Hep27-deficient H1299 cells (Fig. 3B). After 24 h of incubation, cell lysates were immunoprecipitated using mouse monoclonal antibodies targeting either Mdm2 or Hep27. The results of this experiment illustrate reciprocal binding of ectopic Hep27 to Mdm2.

To determine if endogenous Mdm2 could bind to endogenous Hep27, HepG2 cells, which express relatively abundant levels of Hep27, were either treated with the proteasome inhibitor MG132 for 6 h to facilitate Mdm2 protein accumulation or left untreated. Cell lysates were harvested and subjected to overnight immunoprecipitation of endogenous Mdm2 using three different mouse monoclonal antibodies (4B11, 2A10, and SMP14), as well as an anti-Myc antibody (9E10) for use as a negative control (Fig. 3C). Mdm2 in the presence of accumulated protein was capable of pulling down more Hep27 than in the samples with less Mdm2, indicating that Mdm2 and Hep27 interact *in vivo*.

The region of Mdm2 targeted by Hep27 binding was examined by targeting endogenous Hep27 in U2OS cells using a series of N- and C-terminally Myc-tagged Mdm2 deletion mutants. The constructs were transiently transfected into U2OS cells and incubated for 24 h, and IP performed using a mouse anti-Myc monoclonal antibody (Fig. 3D). Ribosomal protein L11 (Rpl11), a protein previously reported to bind amino acids 284 to 374 of Mdm2 (61), was used as a binding control. The binding of Hep27 to Mdm2 deletion mutants closely resembled Rpl11 binding, with negligible binding to Mdm2 amino acids 295 to 491 [Mdm2(295-491)] and Mdm2(1-199). Hep27 binds to all constructs containing amino acids 200 to 294 of Mdm2, the region containing the acidic domain of Mdm2.

Hep27 binding to Mdm2 stabilizes p53. There are a number of small, basic proteins that bind to Mdm2 in the central acidic domain and trigger p53 stabilization. These include the large ribosomal proteins L5, L11, and L23, as well as p14ARF. All of these proteins exhibit tumor suppressor function by acting as negative regulators of Mdm2, indirectly supporting p53 stabilization, accumulation, and subsequent transactivation. Initial experiments did not support a role for Hep27 as a substrate for Mdm2-mediated ubiquitination and degradation (see Fig. S4 in the supplemental material). Consistent with other Mdm2 binding proteins, such as p14ARF and Rpl11, Hep27 is also a basic protein (pI of 8.9 in the mature form) that binds to the central domain of Mdm2; therefore, we investigated the possibility that Hep27 could induce p53 stabilization and accumulation. To this end, cytomegalovirus (CMV)-driven constructs expressing Mdm2, p53, and C-terminally Flag-tagged Hep27 and Hep27-DelN24 were transfected into the p53 null cell line H1299 (Fig. 4A). The introduction of Hep27 and Hep27-DelN24 with Mdm2 alone results in modestly enhanced levels of Mdm2. Coexpression of Hep27 or Hep27-DelN24 leads to significant p53 stabilization and simultaneous accumulation of Mdm2 and p21, which are direct transcriptional targets of p53.

To verify that Hep27 can stabilize endogenous p53 in a physiological setting, where the ratios of Mdm2 and p53 are in a stoichiometric balance, adenovirus expressing C-terminally Flag-tagged Hep27 was used to infect WI-38 cells, which are normal human lung fibroblasts containing wild-type p53 and having no detectable Hep27 expression (Fig. 4B). Increased levels of Hep27 resulted in p53 protein accumulation together with the accumulation of Mdm2 and p21, suggesting increased p53 activity.

Hep27 is transported to and processed in the mitochondria, where it predominantly resides. To determine if the endogenous-p53-stabilizing effects of Hep27 occur outside the mitochondria, Hep27-DelN24-Flag, a mutant lacking the mitochondrial targeting signal, was ectopically expressed in MCF7 cells (Fig. 4C). The protein levels of p53 increased in a dose-depen-

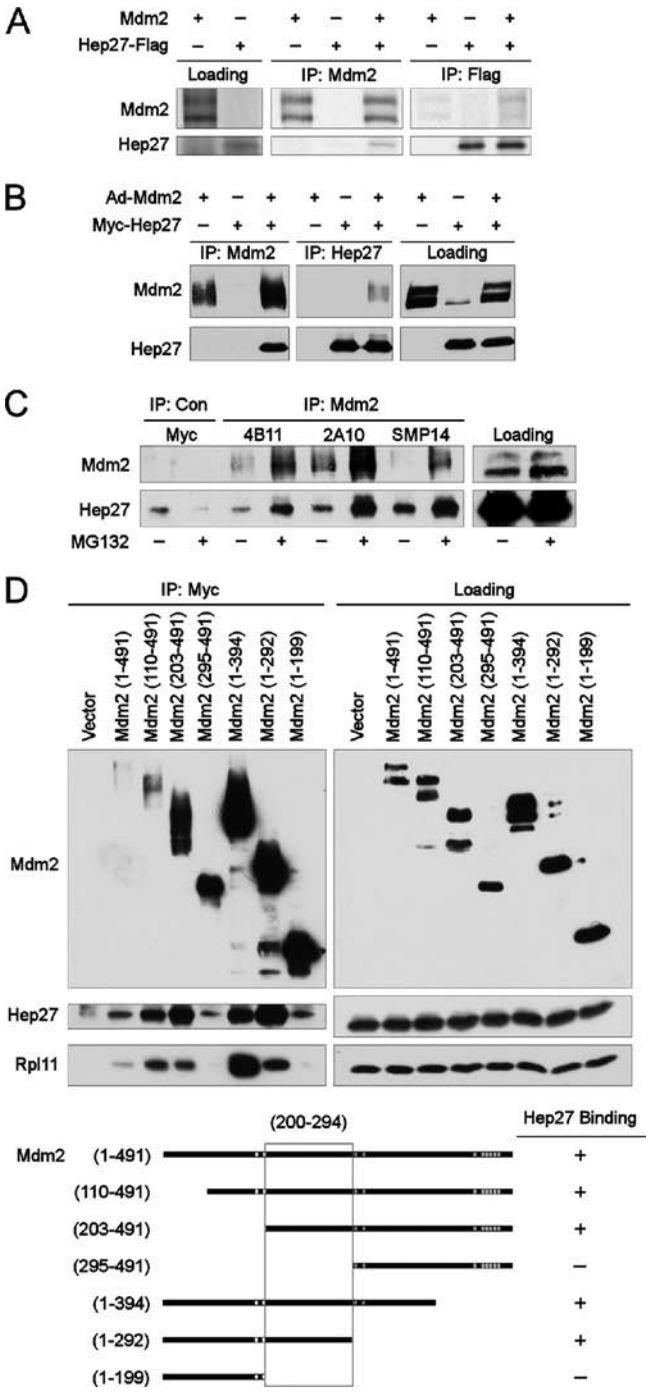

FIG. 3. Hep27 binds to Mdm2. (A) The TNT quick coupled transcription/translation system was used to synthesize [^{35}S]methionine-labeled Mdm2 and Hep27-Flag. Reciprocal immunoprecipitations with anti-Mdm2 2A10 or anti-Flag M2 were detected by Western blot assay. Loading control shows 10% of the starting material. (B) Adenovirus (Ad) constructs expressing Mdm2 or Myc-tagged Hep27 were transduced into H1299 cells. Reciprocal immunoprecipitations with anti-Mdm2 2A10 or anti-Hep27 were detected by Western blot assay. Loading control shows 10% of the starting material. (C) Endogenous Mdm2 and Hep27 were immunoprecipitated from HepG2 cells using control (Con) anti-Myc 9E10 antibody or three different Mdm2 antibodies: 4B11, 2A10, and SMP14. Cells were incubated in the presence or absence of the proteasome inhibitor MG132 for six hours prior to IP. Loading control shows 10% of the starting material. (D) Expression constructs expressing Myc-tagged wild-type and C- or N-terminal Mdm2 truncation mutants were transfected into U2OS cells. Mdm2 constructs were immunoprecipitated with anti-Myc 9E10 antibody, and proteins detected by Western blot assay. Endogenous Rpl11 was used as an Mdm2 binding control. The loading control shows 10% of the starting material. The schematic (bottom) summarizes the experimental evidence that narrows Hep27 binding to Mdm2 amino acids 200 to 294.

dent fashion with Hep27-DelN24 expression, suggesting that the interaction likely occurs in the nucleus. Since overexpression of Hep27 was able to stabilize p53, we next investigated whether reducing the Hep27 protein levels could reduce p53 levels in nonstressed cells. Knocking down endogenous levels of Hep27 with two different RNAi sequences in both MCF7 and U2OS cells reduced the basal levels of p53 (Fig. 4D), suggesting that endogenous Hep27 expression in the absence of stress is important to maintain basal p53 levels. The elevation of basal p53 levels by Hep27 may have important implications in terms of priming cells for apoptosis or enhancing p53 activity under physiological stress conditions. In summary, these results indicate that Hep27 binding to Mdm2 can stabilize p53 in a dose-dependent manner correlating with the level of p53 target gene expression.

The proto-oncogene c-Myb regulates Hep27. The results of previous gene microarray experiments indicated that one member of the Myb family, c-Myb, could induce increased Hep27 transcript levels (22, 24, 43). Ectopic expression of wild-type human c-Myb in WI-38 cells induced an average 58-fold increase in Hep27 transcript levels (Fig. 5A), supporting the notion that c-Myb can promote Hep27 transcription. The c-Myb-induced increase in Hep27 transcript levels correlated with an increase in Hep27 protein levels in WI-38 cells (Fig. 5B), indicating that c-Myb increases Hep27 in a dose-dependent fashion. In contrast, stable knockdown of c-Myb in MCF7 cells resulted in undetectable levels of Hep27 protein compared to the results for a control GFP knockdown (Fig. 5C), signifying a tight correlation between c-Myb and Hep27 expression.

The subset of direct c-Myb target genes is poorly defined and may vary largely by cell type and lineage and cofactor specificity, as well as temporal and spatial expression patterns (33). A number of human genes, including adenosine deaminase (*ADA*), *c-Myc*, and *MAT2A*, have been reported to contain c-Myb sites within their promoter regions (2). In order to determine if Hep27 is a direct c-Myb target gene, regions within the promoter were systematically queried for the c-Myb consensus site [(C/T)AAC(G/T)G] (15). Two putative Myb response elements (MRE) at nucleotides −143 to −138 (MRE A, plus strand, AAACGG) and −39 to −34 (MRE B, minus strand, TAACTG) upstream of the transcription start site (TSS) are consistent with potential c-Myb promoter binding sites (Fig. 5D). To assess the functional nature of these possible promoter sequences, regions within nucleotides −400 to −1 of the TSS were amplified from U2OS genomic DNA and cloned 5′ of the Luc gene in pGL3-Basic to map a minimal promoter region. Constructs P1DelB and P1DelAB are missing putative MREs B and AB, respectively, whereas construct P1AB is a minimal region containing both MREs A and B. The

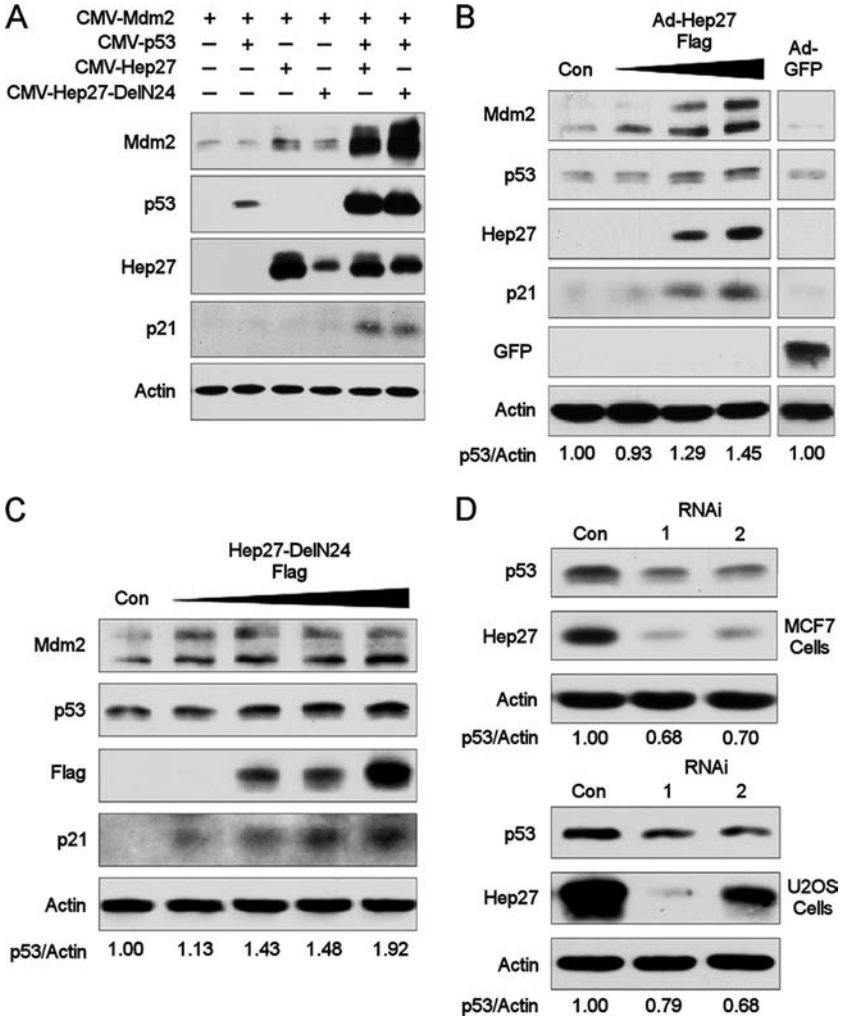

FIG. 4. Hep27 binding to Mdm2 results in p53 stabilization. (A) Expression constructs expressing Mdm2, p53, Hep27, and Hep27-DelN24 were coexpressed in H1299 cells by transient transfection for 24 hours, and indicated proteins detected by Western blot assay. (B) Adenovirus (Ad) construct expressing Hep27-Flag was transduced into WI-38 primary fibroblasts for 24 hours, and indicated proteins detected by Western blot assay. (C) Hep27-DelN24 was transiently expressed in MCF7 cells for 24 hours, and indicated proteins detected by Western blot assay. (D) Two independent oligonucleotides were used to knock down Hep27 in MCF7 and U2OS cells. Endogenous Hep27 and p53 were assessed by Western blot assay. Con, control.

reporter constructs were transiently expressed in H1299 cells in the presence or absence of c-Myb coexpression, and activity assessed as relative light units (RLU) (Fig. 5E). c-Myb-induced P1 activity was attenuated in cells expressing P1DelB and completely abolished in cells expressing P1DelAB. Reporter activity was nearly restored in cells expressing P1AB, identifying nucleotides −151 to −1 of the TSS as the c-Myb-dependent minimal promoter. To further investigate the necessity of MRE A and MRE B, site-directed mutagenesis was utilized to delete portions of each respective response element (Fig. 5D). Deletion of either MRE A or MRE B alone was sufficient to reduce c-Myb-dependent activity. In addition, the loss of both response elements conferred near-baseline levels of activity (Fig. 5F). Together, these results suggest that the Hep27 minimal promoter region of 151 nucleotides contains two Myb response elements that cooperate with one another to support maximal and direct c-Myb induction of Hep27 transcription.

c-Myb stabilizes p53 in a Hep27-dependent manner. The well-established paradigm for oncogenic signaling to p53 involves upregulation of the tumor suppressor p14ARF in response to aberrant activity of activated RAS, c-Myc, and E2F. Given the distinct function of p53 in monitoring oncogenic activity, we set out to determine if overexpressed c-Myb could also stabilize p53. Transient expression of c-Myb in wild-type-p53 MCF7 cells stabilized p53 in a dose-dependent fashion (Fig. 6A). The increase in p53 correlated with a parallel increase in Hep27 protein levels that is also consistent with the induction of p21. To determine if there was a connection between c-Myb-induced Hep27 levels and increased stability of p53, Hep27 levels were knocked down in MCF7 cells and their response to c-Myb expression was assessed (Fig. 6B). c-Myb induced a dose-dependent p53 stabilization and a corresponding increase of p21 in the control scrambled short interfering RNA (siRNA) sample. In contrast, knockdown of Hep27 im-

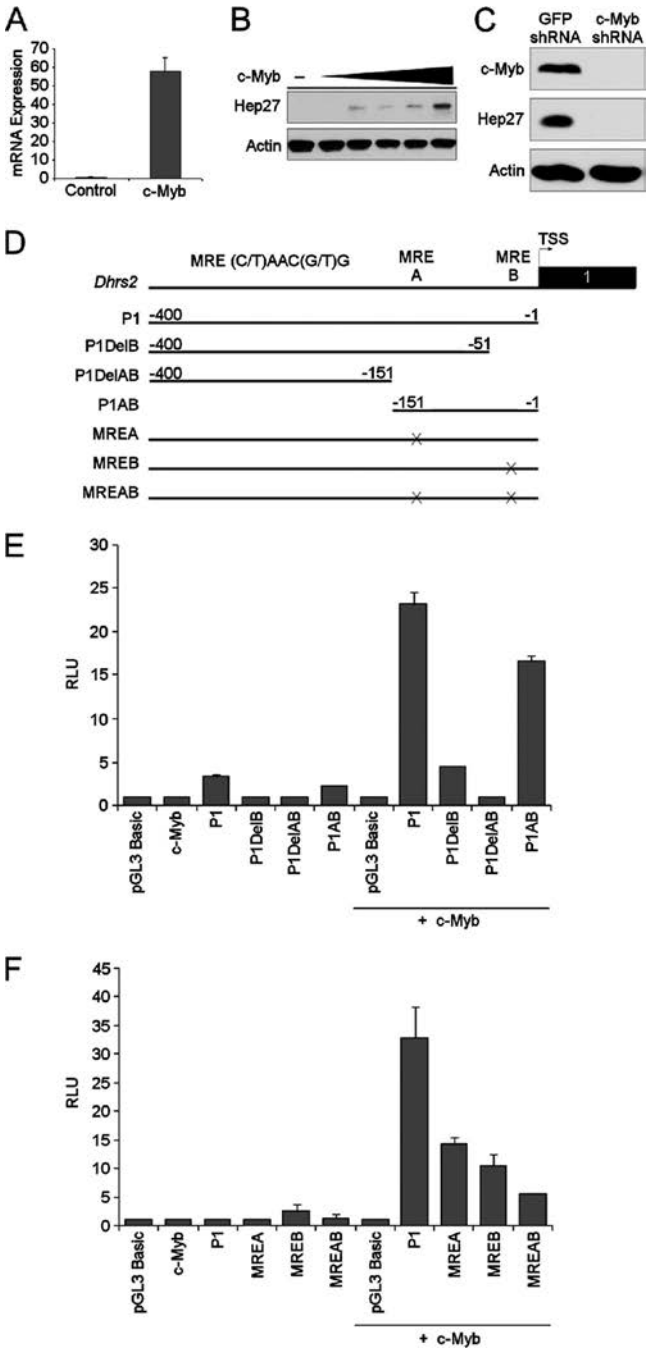

FIG. 5. The proto-oncogene c-Myb regulates Hep27 expression. (A) WI-38 fibroblasts transfected with control vector or c-Myb expression construct were incubated for 36 hours. mRNA was harvested and reverse transcribed for qRT-PCR analysis targeting exons 1 and 2. Results are presented as expression levels of Hep27 relative to that of GAPDH control. (B) c-Myb expression construct was used to transfect WI-38 cells for 36 hours. Anti-Hep27 antibody was used to detect Hep27 expression by Western blot assay. (C) Short hairpin RNA constructs targeting GFP or c-Myb were used to establish stable MCF7 cell lines. Anti-c-Myb and anti-Hep27 antibodies were used to detect endogenous c-Myb and Hep27 levels by Western blot assay. (D) Schematic illustrating putative c-Myb response elements in the promoter of the Hep27 gene (*DHRS2*). The consensus Myb response element (MRE) is shown. Constructs for the minimal promoter mapping and site-directed mutagenesis are shown. (E and F) Luciferase reporter constructs were transfected into H1299 cells in the presence and absence of c-Myb coexpression for 48 hours. pGL3 Basic and c-Myb were transfected alone as controls, and β-galactosidase expressed with all samples as a transfection control. Relative light units (RLU) represent the relative expression of the luciferase/β-galactosidase ratio. Error bars represent standard errors of the means.

paired c-Myb-induced p53 stabilization and diminished p21 accumulation. Moreover, stable knockdown of c-Myb in MCF7 cells resulted in decreased Hep27 levels and p53 levels, indicating that physiological levels of c-Myb expression stabilize p53 (Fig. 6C). c-Myb induced higher levels of Hep27 overall, resulting in increased nuclear levels of mature Hep27 (Fig. 6D). Together, this evidence suggests that c-Myb-induced Hep27 expression is required for the p53-stabilizing effects of c-Myb. The data provide evidence for a c-Myb-Hep27-Mdm2-p53 pathway. c-Myb induction of Hep27 promotes mitochondrial matrix accumulation of the mature protein. A fraction of Hep27 is translocated to the nucleus, leading to the inhibition of Mdm2 and subsequent stabilization of p53 (Fig. 6E).

A potential ER-c-Myb-Hep27-Mdm2-p53 pathway in breast cancer. Our *in vitro* analyses have identified a mechanism for the involvement of Hep27 in the p53 pathway through c-Myb signaling. To determine if this pathway has any relevance for human breast cancer patients, we analyzed a well-studied breast tumor microarray data set (28) ($n = 236$) representing a large cohort of patient samples that contains survival data, p53 mutation status, and estrogen receptor (ER) status. Tumors were classified into intrinsic subtypes (basal-like, HER2-enriched, luminal A, luminal B, and normal-like) using the PAM50 subtype predictor as described in reference 35, and disease-specific survival was analyzed using the Kaplan-Meier estimator (Fig. 7A). Survival outcome across subtypes in this data set was similar to that of other previously analyzed breast tumor microarray datasets (53) and, therefore, is appropriate for use in this study. With stratification of samples by ER status, the expression of Hep27 was determined to be significantly higher in the ER-positive (ER^+) tumors (Fig. 7B). This is consistent with a role for direct ER regulation of c-Myb (9) and supports the notion that ER-induced c-Myb stimulates increased expression of Hep27 (see Fig. S5 in the supplemental material). The transcript levels of both c-Myb and Hep27 were shown to vary significantly across the breast tumor subtypes (Fig. 7C and D) in a manner consistent with ER status (i.e., highest in the ER^+ subtypes of luminal A and B). Both c-Myb and Hep27 expression levels were lowest in the typically ER-negative (ER^-) basal-like tumors. Hep27 expression levels were also high in the subset of HER2-enriched tumors, many of which were ER^+ (37/50) and all of which showed some luminal cell characteristics.

The p53 mutation frequency among the intrinsic subtypes tends to be high among the basal-like, Her2-enriched, and luminal B tumors but low within luminal A tumors (52), a pattern also observed within this data set (data not shown). Higher Hep27 expression was significantly associated with wild-type-p53 tumors (Fig. 7E) in a manner consistent with elevated Hep27 expression in the luminal A subtype. To assess the p53 functional status, we applied a gene signature capable of predicting nonfunctional p53 (p53 mutation signature) (56)

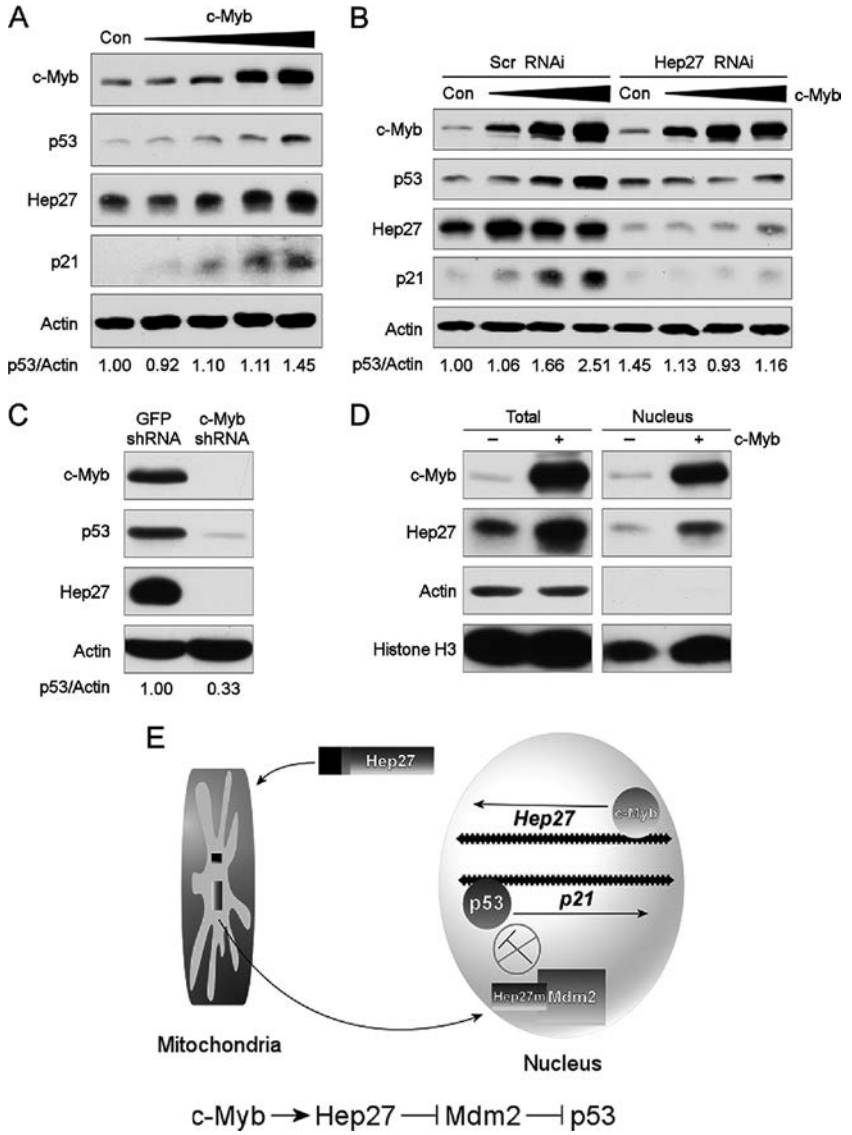

FIG. 6. c-Myb induces p53 stabilization and activation in a Hep27-dependent manner. (A) Expression construct expressing c-Myb was transfected into MCF7 cells for 24 hours, and indicated proteins were detected by Western blot assay. Con, control. (B) Scrambled (Scr) RNAi and Hep27 oligonucleotides were transfected into MCF7 cells and incubated for 48 hours. Cells were washed, and an additional transfection performed with a c-Myb expression construct. Cells were incubated for an additional 24 hours and harvested for Western blot assay. (C) Short hairpin RNA constructs targeting GFP or c-Myb were used to establish stable MCF7 cell lines. Endogenous c-Myb, Hep27, and p53 levels were detected by Western blot assay. (D) Expression construct for c-Myb was transfected into MCF7 cells for 24 hours. Whole-cell lysate (Total) and the nuclear fraction (Nucleus) were assessed by Western blot assay. Actin is a cytosolic control, and histone H3 is a nuclear control. (E) Model for c-Myb-Hep27-Mdm2-p53 signaling. The proto-oncogene c-Myb induces the expression of full-length Hep27 preprotein. Hep27 is actively imported to the mitochondria by an N-terminal mitochondrial targeting signal (MTS). Once the protein is imported into the mitochondrial matrix, the MTS is cleaved off to produce mature Hep27 (Hep27m). A minor fraction of Hep27m translocates to the nucleus to bind to Mdm2, resulting in p53 stabilization and subsequent transactivation of downstream target genes.

to the Miller data set and found the mutation signature to be lowest in the luminal A tumors, indicative of a functional p53 pathway within this subtype (Fig. 7F). We performed comparable tests on two other breast cancer datasets that did not have as complete a set of clinical and genomic data (i.e., the UNC [16a] and NKI [57a] data sets, both lacking p53 mutation status) and observed similar results (data not shown). Together, these *in vivo* correlations suggest that, due to c-Myb regulation of Hep27, the ER^+ luminal A breast cancer subtype has high c-Myb and Hep27 levels. In addition, the ER^+ luminal A tumors with high Hep27 levels tend to be associated with functional, wild-type p53 and overall better survival. This supports the possibility that an ER-c-Myb-Hep27-Mdm2-p53 pathway may modulate p53 function in luminal breast tumor subtypes, in particular, luminal A tumors.

DISCUSSION

Posttranslational inhibition of Mdm2 is an important means of modulating p53 function in response to a number of cellular

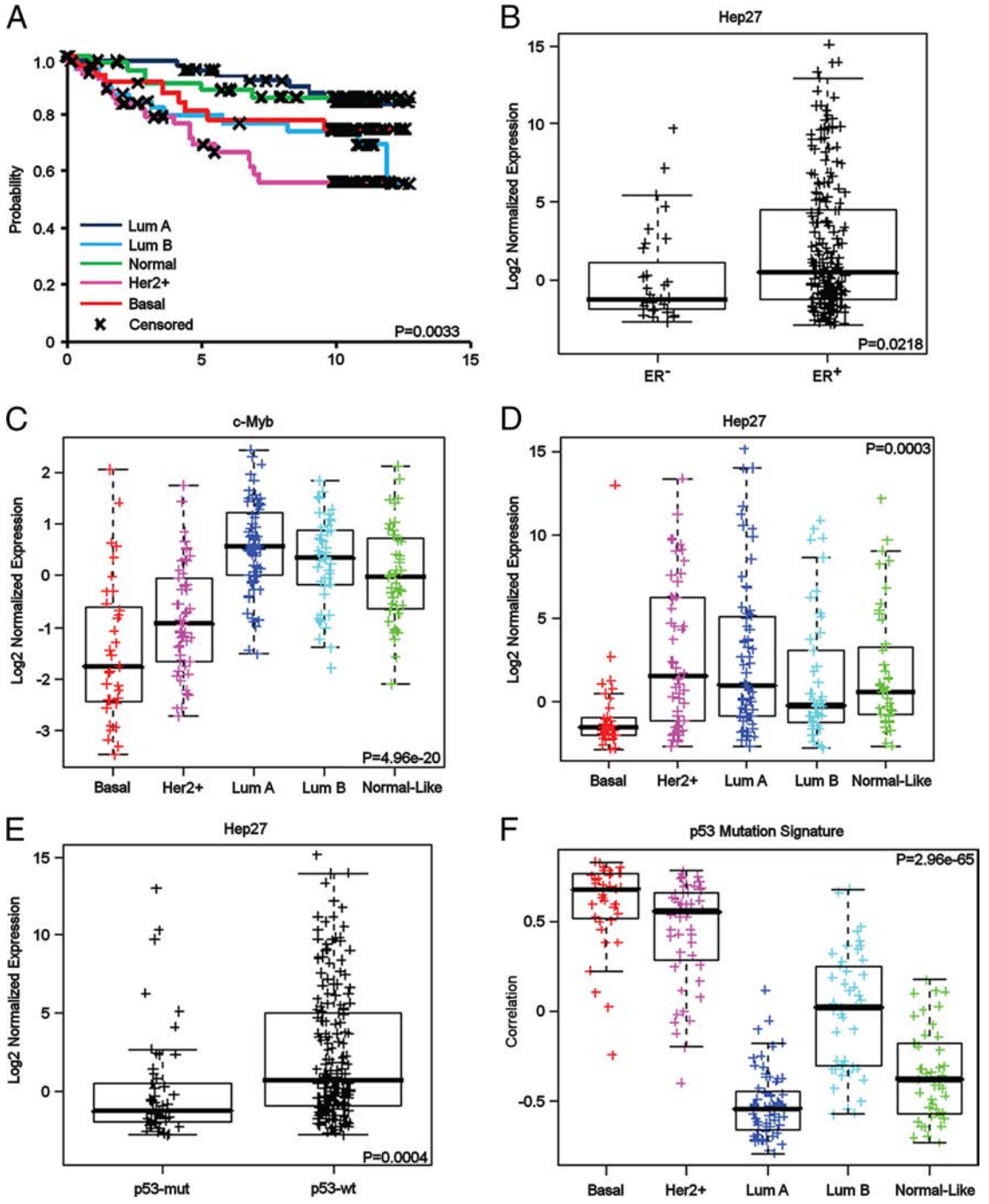

FIG. 7. A potential c-Myb-Hep27-Mdm2-p53 pathway in breast cancer. The Miller et al. dataset ($n = 236$) (28) was classified into the breast tumor-intrinsic subtypes (basal-like, HER2-enriched, luminal [Lum] A, luminal B, and normal-like) using the PAM50 predictor (35). (A) Kaplan-Meier survival analysis of disease-specific survival stratified by subtype. *P* value was determined by log-rank test, testing the null hypothesis that the survival curves are identical across the subtypes. (B) Hep27 mRNA expression in ER^- and ER^+ tumors ($n = 232$). *P* values calculated by *t* test show different expression values across ER status or biologically defined breast tumor subtypes. (C) c-Myb and (D) Hep27 expression varies by intrinsic subtype. *P* values were determined by ANOVA, testing the null hypothesis that all group means are equal. (E) Hep27 expression in mutant-p53 (mut) and wild-type-p53 (wt) tumors. *P* values calculated by *t* test show different expression values across ER status or biologically defined breast tumor subtypes. (F) A p53 mutation signature (56) was applied to this dataset and correlated with breast tumor subtype. *P* values were determined by ANOVA, testing the null hypothesis that all group means are equal. For box and whisker plots, the horizontal bars represent the medians, the lower and upper hinges of the boxes represent the first and third quartiles, and the whiskers extend to $\pm 1.58 \times$ interquartile range/$\sqrt{n}$.

insults, including nucleolar and mitogenic stress. The intermediate mediators of these Mdm2 regulatory pathways include the large ribosomal proteins L5, L11, and L23, as well as the tumor suppressor p14ARF. All of these small basic proteins are localized primarily to the nucleolus, maintaining close proximity to Mdm2. Here, we demonstrate that mitochondrial protein Hep27, another small basic protein, can bind to Mdm2 and promote p53 stabilization. Like many mitochondrial proteins, synthesis of nuclear-encoded Hep27 occurs in the cytoplasm, followed by translocation and import into the mitochondrial matrix, where cleavage of the mitochondrial targeting signal occurs to generate mature Hep27. The mature protein accumulates primarily in the mitochondria, potentially performing "housekeeping" functions on unknown substrates within the matrix space. Previous screening for potential mitochondrial substrates of Hep27 suggested an NADPH-dependent carbonyl reductase function (46). Further experimentation is necessary to determine the precise mitochondrial function of Hep27.

As a mitochondrial matrix protein, it seems counterintuitive that a protein with native functions in the mitochondria could impart functions elsewhere in the cell. However, it is estimated that 10% or more of mitochondrial proteins exhibit dual subcellular locations (34, 48), and there is mounting evidence to support extramitochondrial functions for nuclear-encoded mitochondrial matrix proteins (51). Much like Hep27, Hsp60 contains an N-terminal mitochondrial targeting signal that directs newly synthesized Hsp60 to the mitochondrial matrix, where the signal peptide undergoes cleavage to generate the mature form of the protein. This mature form of Hsp60 has been documented to localize in the endoplasmic reticulum, plasma membrane, and peroxisomes, where it may function as a chaperone for nonmitochondrial proteins (20, 50). Mitochondrial Hsp70 is yet another protein that is localized to the cytoplasm, where it contributes to cellular senescence (58). Given the critical importance of mitochondria as dynamic integrators of signaling events related to cell proliferation, nutrient sensing, energy, and metabolism (reviewed in reference 14, 44), it will be interesting to explore other possible mitochondrial matrix proteins that may be involved in mitochondria-to-nucleus signaling.

Our data demonstrate that mature Hep27 is partially translocated from the mitochondria to the nucleus. Nuclear-localized Hep27 binds to Mdm2 and promotes p53 stabilization. The connection between aberrantly high expression of c-Myb and the activation of p53 supports a model for an oncogene-tumor suppressor loop, where p53 monitors the activity of c-Myb via Hep27. Indeed, activated p53 has been reported to form a ternary complex with the corepressor mSin3A and c-Myb, resulting in the inhibition of c-Myb transcriptional activity (55). Moreover, p53 activation can also stimulate c-Myb proteasomal degradation in a Siah-dependent fashion (54). Collectively, these data provide evidence for a negative-feedback loop between c-Myb and p53, where deregulated c-Myb can promote Hep27-dependent p53 activation, in turn resulting in downregulation of both c-Myb protein levels and transactivation potential.

The mechanism underlying the translocation of Hep27 from the mitochondrial matrix to the nucleus is unclear. A recent study describes vesicular carriers, termed mitochondrion-derived vesicles (MDV), that can selectively transport cargo derived from all mitochondrial compartments to peroxisomes (32). Interestingly, Hep27 has also been reported to localize to peroxisomes via a C-terminal peroxisomal targeting signal (16). Given the importance of vesicular trafficking within the cell to relay biochemical messages from various subcellular compartments, it is tempting to speculate that mitochondrion-derived vesicles can selectively transport mature Hep27 from the mitochondria to other observed locations, like peroxisomes and the nucleus. Further investigation is warranted to determine the exact nature of Hep27 translocation from the mitochondria to the nucleus.

The connection between c-Myb and oncogenesis entails documented overexpression of c-Myb in a number of hematopoietic malignancies, breast cancer, and colon cancer, as well as some melanoma, pancreatic, and esophageal cancers (39, 40). Given the role of c-Myb in promoting cell growth and proliferation, it is reasonable to expect that c-Myb may play a functional role in promoting or maintaining a malignant phenotype. At this time, it is unclear if the Hep27 locus or gene expression levels are altered in any way within c-Myb-dependent tumor types.

By analyzing human breast tumor microarray data, we observed Hep27 expression to be highest in ER^+ and wild-type-p53 tumors, phenotypes characteristic of the luminal A subtype. Indeed, both c-Myb and Hep27 have increased expression in the luminal A subtype relative to their levels of expression in the basal-like subtype, the latter being a subtype with tumors that frequently are ER^- and have mutated p53. Using a gene signature capable of predicting nonfunctional p53, the luminal A samples had the lowest expression of a p53 mutation signature, indicative of normal p53 function. These data suggest that the proposed c-Myb-Hep27-Mdm2-p53 pathway may exist *in vivo* and be functional in ER^+ luminal A tumors but not basal-like breast cancers. With an ER-c-Myb-Hep27-Mdm2-p53 axis intact, these correlative findings could, in part, explain the relative chemotherapy insensitivity of luminal A cancers (35, 42). Due to potential Hep27-mediated stabilization of p53, the luminal A tumor response to chemotherapy may result in a p53-mediated cell cycle arrest and subsequent cytotoxic insensitivity.

Cross talk between the estrogen receptor and p53 has previously been suggested. T47D human breast cancer cells, containing a mutant form of p53, restored elevated p53 levels following treatment with estradiol (17). In addition, wild-type-p53 MCF7 breast cancer cell lines overexpressing Mdm2 demonstrated increased steady-state levels of p53 in the presence of estradiol (45). Studies using murine models assessing estrogen stimulation of the mammary gland not only reported increased levels of nuclear, functional p53 (21, 49) but also demonstrated that hormone stimulation is necessary for a maximal p53-mediated response to ionizing radiation (1). Finally, wild-type p53 but not mutant p53 was found to bind to the estrogen receptor *in vivo* and repress ER-dependent transcriptional activity (60). An ER-dependent c-Myb-Hep27-Mdm2-p53 pathway could provide a molecular link between ER activation and p53 stabilization in cells of the mammary gland. ER modulation of p53 could, in turn, result in p53-dependent downregulation of ER activity, supporting a negative-feedback loop between the two.

Evidence has been presented for a novel Mdm2 regulatory pathway involving c-Myb induction of the mitochondrial protein Hep27. Elevated expression of c-Myb promotes nuclear accumulation of Hep27, which is able to support p53 stabilization and activation. A c-Myb-Hep27-Mdm2-p53 pathway may not only have implications in c-Myb-dependent cancers but may also play a potential role in physiological regulation of cell cycle dynamics during development and hematopoiesis, areas where c-Myb is known to play a critical role. Furthermore, this work sheds light on signaling pathways involved in cross-talk communication between the mitochondria and nucleus. Future investigation will aim at elucidating the roles of Hep27 in mitochondrial dynamics and metabolism, cell cycle regulation, and tumor suppressor function.

ACKNOWLEDGMENTS

We thank Mikael Lindstrom, Koji Itahana, Everardo Macias, and Aiwen Jin for their helpful advice and technical assistance. Scott Ness generously provided c-Myb adenovirus for initial experiments.

Y.Z. is a recipient of a Career Award in Biomedical Science from the Burroughs Wellcome Fund, Howard Temin Award from the National Cancer Institute, and Scholar Award from the Leukemia & Lymphoma Society. This study was supported by grants from the NIH and the American Cancer Society to Y.Z. and by an NCI Breast SPORE grant and support from the Breast Cancer Research Foundation to C.M.P.

REFERENCES

1. **Becker, K. A., S. Lu, E. S. Dickinson, K. A. Dunphy, L. Mathews, S. S. Schneider, and D. J. Jerry.** 2005. Estrogen and progesterone regulate radiation-induced p53 activity in mammary epithelium through TGF-beta-dependent pathways. Oncogene **24:**6345–6353.
2. **Berge, T., V. Matre, E. M. Brendeford, T. Saether, B. Luscher, and O. S. Gabrielsen.** 2007. Revisiting a selection of target genes for the hematopoietic transcription factor c-Myb using chromatin immunoprecipitation and c-Myb knockdown. Blood Cells Mol. Dis. **39:**278–286.
3. **Bjorkqvist, A. M., M. Wolf, S. Nordling, L. Tammilehto, A. Knuuttila, J. Kere, K. Mattson, and S. Knuutila.** 1999. Deletions at 14q in malignant mesothelioma detected by microsatellite marker analysis. Br. J. Cancer **81:**1111–1115.
4. **Cheng, Y., J. M. Ko, H. L. Lung, P. H. Lo, E. J. Stanbridge, and M. L. Lung.** 2003. Monochromosome transfer provides functional evidence for growth-suppressive genes on chromosome 14 in nasopharyngeal carcinoma. Genes Chromosomes Cancer **37:**359–368.
5. **Claros, M. G., and P. Vincens.** 1996. Computational method to predict mitochondrially imported proteins and their targeting sequences. Eur. J. Biochem. **241:**779–786.
6. **Dai, M. S., and H. Lu.** 2004. Inhibition of MDM2-mediated p53 ubiquitination and degradation by ribosomal protein L5. J. Biol. Chem. **279:**44475–44482.
7. **Debiec-Rychter, M., R. Sciot, P. Pauwels, E. Schoenmakers, P. Dal Cin, and A. Hagemeijer.** 2001. Molecular cytogenetic definition of three distinct chromosome arm 14q deletion intervals in gastrointestinal stromal tumors. Genes Chromosomes Cancer **32:**26–32.
8. **Donadel, G., C. Garzelli, R. Frank, and F. Gabrielli.** 1991. Identification of a novel nuclear protein synthesized in growth-arrested human hepatoblastoma HepG2 cells. Eur. J. Biochem. **195:**723–729.
9. **Drabsch, Y., H. Hugo, R. Zhang, D. H. Dowhan, Y. R. Miao, A. M. Gewirtz, S. C. Barry, R. G. Ramsay, and T. J. Gonda.** 2007. Mechanism of and requirement for estrogen-regulated MYB expression in estrogen-receptor-positive breast cancer cells. Proc. Natl. Acad. Sci. U. S. A. **104:**13762–13767.
10. **El-Rifai, W., M. Sarlomo-Rikala, L. C. Andersson, M. Miettinen, and S. Knuutila.** 2000. High-resolution deletion mapping of chromosome 14 in stromal tumors of the gastrointestinal tract suggests two distinct tumor suppressor loci. Genes Chromosomes Cancer **27:**387–391.
11. **Emanuelsson, O., H. Nielsen, S. Brunak, and G. von Heijne.** 2000. Predicting subcellular localization of proteins based on their N-terminal amino acid sequence. J. Mol. Biol. **300:**1005–1016.
12. **Gabrielli, F., G. Donadel, G. Bensi, A. Heguy, and M. Melli.** 1995. A nuclear-protein, synthesized in growth-arrested human hepatoblastoma cells, is a novel member of the short-chain alcohol-dehydrogenase family. Eur. J. Biochem. **232:**473–477.
13. **Goeze, A., K. Schluns, G. Wolf, Z. Thasler, S. Petersen, and I. Petersen.** 2002. Chromosomal imbalances of primary and metastatic lung adenocarcinomas. J. Pathol. **196:**8–16.
14. **Goldenthal, M. J., and J. Marin-Garcia.** 2004. Mitochondrial signaling pathways: a receiver/integrator organelle. Mol. Cell. Biochem. **262:**1–16.
15. **Gonda, T. J.** 1998. The c-Myb oncoprotein. Int. J. Biochem. Cell Biol. **30:**547–551.
16. **Hawkins, J., D. Mahony, S. Maetschke, M. Wakabayashi, R. D. Teasdale, and M. Boden.** 2007. Identifying novel peroxisomal proteins. Proteins **69:**606–616.

16a. **Herschkowitz, J. I., et al.** 2007. Identification of conserved gene expression features between murine mammary carcinoma models and human breast tumors. Genome Biol. **8:**R76.

17. **Hurd, C., N. Khattree, P. Alban, K. Nag, S. C. Jhanwar, S. Dinda, and V. K. Moudgil.** 1995. Hormonal regulation of the p53 tumor suppressor protein in T47D human breast carcinoma cell line. J. Biol. Chem. **270:**28507–28510.
18. **Jin, A., K. Itahana, K. O'Keefe, and Y. Zhang.** 2004. Inhibition of HDM2 and activation of p53 by ribosomal protein L23. Mol. Cell. Biol. **24:**7669–7680.
19. **Jornvall, H., B. Persson, M. Krook, S. Atrian, R. Gonzalez-Duarte, J. Jeffery, and D. Ghosh.** 1995. Short-chain dehydrogenases/reductases (SDR). Biochemistry **34:**6003–6013.
20. **Khan, I. U., R. Wallin, R. S. Gupta, and G. M. Kammer.** 1998. Protein kinase A-catalyzed phosphorylation of heat shock protein 60 chaperone regulates its attachment to histone 2B in the T lymphocyte plasma membrane. Proc. Natl. Acad. Sci. U. S. A. **95:**10425–10430.
21. **Kuperwasser, C., J. Pinkas, G. D. Hurlbut, S. P. Naber, and D. J. Jerry.** 2000. Cytoplasmic sequestration and functional repression of p53 in the mammary epithelium is reversed by hormonal treatment. Cancer Res. **60:**2723–2729.
22. **Lei, W. L., J. J. Rushton, L. M. Davis, F. Liu, and S. A. Ness.** 2004. Positive and negative determinants of target gene specificity in Myb transcription factors. J. Biol. Chem. **279:**29519–29527.
23. **Levine, A. J.** 1997. p53, the cellular gatekeeper for growth and division. Cell **88:**323–331.
24. **Liu, F., W. Lei, J. P. O'Rourke, and S. A. Ness.** 2006. Oncogenic mutations cause dramatic, qualitative changes in the transcriptional activity of c-Myb. Oncogene **25:**795–805.
25. **Lohrum, M. A., R. L. Ludwig, M. H. Kubbutat, M. Hanlon, and K. H. Vousden.** 2003. Regulation of HDM2 activity by the ribosomal protein L11. Cancer Cell **3:**577–587.
26. **Maya, R., M. Balass, S. T. Kim, D. Shkedy, J. F. Leal, O. Shifman, M. Moas, T. Buschmann, Z. Ronai, Y. Shiloh, M. B. Kastan, E. Katzir, and M. Oren.** 2001. ATM-dependent phosphorylation of Mdm2 on serine 395: role in p53 activation by DNA damage. Genes Dev. **15:**1067–1077.
27. **Mayo, L. D., J. J. Turchi, and S. J. Berberich.** 1997. Mdm-2 phosphorylation by DNA-dependent protein kinase prevents interaction with p53. Cancer Res. **57:**5013–5016.
28. **Miller, L. D., J. Smeds, J. George, V. B. Vega, L. Vergara, A. Ploner, Y. Pawitan, P. Hall, S. Klaar, E. T. Liu, and J. Bergh.** 2005. An expression signature for p53 status in human breast cancer predicts mutation status, transcriptional effects, and patient survival. Proc. Natl. Acad. Sci. U. S. A. **102:**13550–13555.
29. **Mutirangura, A., W. Pornthanakasem, V. Sriuranpong, P. Supiyaphun, and N. Voravud.** 1998. Loss of heterozygosity on chromosome 14 in nasopharyngeal carcinoma. Int. J. Cancer. **78:**153–156.
30. **Ness, S. A.** 1996. The Myb oncoprotein: regulating a regulator. Biochim. Biophys. Acta **1288:**F123–F139.
31. **Ness, S. A.** 2003. Myb protein specificity: evidence of a context-specific transcription factor code. Blood Cells Mol. Dis. **31:**192–200.
32. **Neuspiel, M., A. C. Schauss, E. Braschi, R. Zunino, P. Rippstein, R. A. Rachubinski, M. A. Andrade-Navarro, and H. M. McBride.** 2008. Cargo-selected transport from the mitochondria to peroxisomes is mediated by vesicular carriers. Curr. Biol. **18:**102–108.
33. **Oh, I. H., and E. P. Reddy.** 1999. The myb gene family in cell growth, differentiation and apoptosis. Oncogene **18:**3017–3033.
34. **Pagliarini, D. J., S. E. Calvo, B. Chang, S. A. Sheth, S. B. Vafai, S. E. Ong, G. A. Walford, C. Sugiana, A. Boneh, W. K. Chen, D. E. Hill, M. Vidal, J. G. Evans, D. R. Thorburn, S. A. Carr, and V. K. Mootha.** 2008. A mitochondrial protein compendium elucidates complex I disease biology. Cell **134:**112–123.
35. **Parker, J. S., M. Mullins, M. C. Cheang, S. Leung, D. Voduc, T. Vickery, S. Davies, C. Fauron, X. He, Z. Hu, J. F. Quackenbush, I. J. Stijleman, J. Palazzo, J. S. Marron, A. B. Nobel, E. Mardis, T. O. Nielsen, M. J. Ellis, C. M. Perou, and P. S. Bernard.** 2009. Supervised risk predictor of breast cancer based on intrinsic subtypes. J. Clin. Oncol. **27:**1160–1167.
36. **Pellegrini, S., S. Censini, S. Guidotti, P. Iacopetti, M. Rocchi, M. Bianchi, A. Covacci, and F. Gabrielli.** 2002. A human short-chain dehydrogenase/reductase gene: structure, chromosomal localization, tissue expression and subcellular localization of its product. Biochem. Biophys. Acta Gene Struct. Expr. **1574:**215–222.
37. **Petropavlovskaia, M., C. A. Bodnar, L. A. Behie, and L. Rosenberg.** 2006. Pancreatic small cells: analysis of quiescence, long-term maintenance and insulin expression in vitro. Exp. Cell Res. **30:**30.
38. **Pfanner, N.** 2000. Protein sorting: recognizing mitochondrial presequences. Curr. Biol. **10:**R412–R415.

39. **Ramsay, R. G.** 2005. c-Myb a stem-progenitor cell regulator in multiple tissue compartments. Growth Factors **23:**253–261.
40. **Ramsay, R. G., and T. J. Gonda.** 2008. MYB function in normal and cancer cells. Nat. Rev. Cancer **8:**523–534.
41. **Ramsby, M. L., and G. S. Makowski.** 1999. Differential detergent fractionation of eukaryotic cells. Analysis by two-dimensional gel electrophoresis. Methods Mol. Biol. **112:**53–66.
42. **Rouzier, R., C. M. Perou, W. F. Symmans, N. Ibrahim, M. Cristofanilli, K. Anderson, K. R. Hess, J. Stec, M. Ayers, P. Wagner, P. Morandi, C. Fan, I. Rabiul, J. S. Ross, G. N. Hortobagyi, and L. Pusztai.** 2005. Breast cancer molecular subtypes respond differently to preoperative chemotherapy. Clin. Cancer Res. **11:**5678–5685.
43. **Rushton, J. J., L. M. Davis, W. Lei, X. Mo, A. Leutz, and S. A. Ness.** 2003. Distinct changes in gene expression induced by A-Myb, B-Myb and c-Myb proteins. Oncogene **22:**308–313.
44. **Ryan, M. T., and N. J. Hoogenraad.** 2007. Mitochondrial-nuclear communications. Annu. Rev. Biochem. **76:**701–722.
45. **Saji, S., S. Nakashima, S. Hayashi, M. Toi, and Y. Nozawa.** 1999. Overexpression of MDM2 in MCF-7 promotes both growth advantage and p53 accumulation in response to estradiol. Jpn. J. Cancer Res. **90:**210–218.
46. **Shafqat, N., J. Shafqat, G. Eissner, H. U. Marschall, K. Tryggvason, U. Eriksson, F. Gabrielli, H. Lardy, H. Jornvall, and U. Oppermann.** 2006. Hep27, a member of the short-chain dehydrogenase/reductase family, is an NADPH-dependent dicarbonyl reductase expressed in vascular endothelial tissue. Cell. Mol. Life Sci. **63:**1205–1213.
47. **Sharpless, N. E., and R. A. DePinho.** 1999. The INK4A/ARF locus and its two gene products. Curr. Opin. Genet. Dev. **9:**22–30.
48. **Sickmann, A., J. Reinders, Y. Wagner, C. Joppich, R. Zahedi, H. E. Meyer, B. Schonfisch, I. Perschil, A. Chacinska, B. Guiard, P. Rehling, N. Pfanner, and C. Meisinger.** 2003. The proteome of Saccharomyces cerevisiae mitochondria. Proc. Natl. Acad. Sci. U. S. A. **100:**13207–13212.
49. **Sivaraman, L., O. M. Conneely, D. Medina, and B. W. O'Malley.** 2001. p53 is a potential mediator of pregnancy and hormone-induced resistance to mammary carcinogenesis. Proc. Natl. Acad. Sci. U. S. A. **98:**12379–12384.
50. **Soltys, B. J., and R. S. Gupta.** 1996. Immunoelectron microscopic localization of the 60-kDa heat shock chaperonin protein (Hsp60) in mammalian cells. Exp. Cell Res. **222:**16–27.
51. **Soltys, B. J., and R. S. Gupta.** 1999. Mitochondrial-matrix proteins at unexpected locations: are they exported? Trends Biochem. Sci. **24:**174–177.
52. **Sorlie, T., C. M. Perou, C. Fan, S. Geisler, T. Aas, A. Nobel, G. Anker, L. A. Akslen, D. Botstein, A. L. Borresen-Dale, and P. E. Lonning.** 2006. Gene expression profiles do not consistently predict the clinical treatment response in locally advanced breast cancer. Mol. Cancer Ther. **5:**2914–2918.
53. **Sorlie, T., R. Tibshirani, J. Parker, T. Hastie, J. S. Marron, A. Nobel, S. Deng, H. Johnsen, R. Pesich, S. Geisler, J. Demeter, C. M. Perou, P. E. Lonning, P. O. Brown, A. L. Borresen-Dale, and D. Botstein.** 2003. Repeated observation of breast tumor subtypes in independent gene expression data sets. Proc. Natl. Acad. Sci. U. S. A. **100:**8418–8423.
54. **Tanikawa, J., E. Ichikawa-Iwata, C. Kanei-Ishii, and S. Ishii.** 2001. Regulation of c-Myb activity by tumor suppressor p53. Blood Cells Mol. Dis. **27:**479–482.
55. **Tanikawa, J., T. Nomura, E. M. Macmillan, T. Shinagawa, W. Jin, K. Kokura, D. Baba, M. Shirakawa, T. J. Gonda, and S. Ishii.** 2004. p53 suppresses c-Myb-induced trans-activation and transformation by recruiting the corepressor mSin3A. J. Biol. Chem. **279:**55393–55400.
56. **Troester, M. A., J. I. Herschkowitz, D. S. Oh, X. He, K. A. Hoadley, C. S. Barbier, and C. M. Perou.** 2006. Gene expression patterns associated with p53 status in breast cancer. BMC Cancer **6:**276.
57. **Truscott, K. N., K. Brandner, and N. Pfanner.** 2003. Mechanisms of protein import into mitochondria. Curr. Biol. **13:**R326–R337.

57a. **van de Vijver, M. J., et al.** 2002. A gene-expression signature as a predictor of survival in breast cancer. N. Engl. J. Med. **347:**1999–2009.

58. **Wadhwa, R., S. C. Kaul, Y. Ikawa, and Y. Sugimoto.** 1993. Identification of a novel member of mouse hsp70 family. Its association with cellular mortal phenotype. J. Biol. Chem. **268:**6615–6621.
59. **Yi, H., J. Leunissen, G. Shi, C. Gutekunst, and S. Hersch.** 2001. A novel procedure for pre-embedding double immunogold-silver labeling at the ultrastructural level. J. Histochem. Cytochem. **49:**279–284.
60. **Yu, C. L., P. Driggers, G. Barrera-Hernandez, S. B. Nunez, J. H. Segars, and S. Cheng.** 1997. The tumor suppressor p53 is a negative regulator of estrogen receptor signaling pathways. Biochem. Biophys. Res. Commun. **239:**617–620.
61. **Zhang, Y. P., G. W. Wolf, K. Bhat, A. Jin, T. Allio, W. A. Burkhart, and Y. Xiong.** 2003. Ribosomal protein L11 negatively regulates oncoprotein MDM2 and mediates a p53-dependent ribosomal-stress checkpoint pathway. Mol. Cell Biol. **23:**8902–8912.